

# Comparative atomic-scale hydration of the ceramide and phosphocholine headgroup in solution and bilayer environments

Cite as: J. Chem. Phys. **144**, 225101 (2016); <https://doi.org/10.1063/1.4952444>

Submitted: 02 March 2016 . Accepted: 12 May 2016 . Published Online: 08 June 2016

Richard J. Gillams, Christian D. Lorenz, and Sylvia E. McLain



View Online



Export Citation



CrossMark

## ARTICLES YOU MAY BE INTERESTED IN

[On the structure of an aqueous propylene glycol solution](#)

The Journal of Chemical Physics **145**, 224504 (2016); <https://doi.org/10.1063/1.4971208>

[On the hydration of the phosphocholine headgroup in aqueous solution](#)

The Journal of Chemical Physics **133**, 145103 (2010); <https://doi.org/10.1063/1.3488998>

[On the solvation structure of dimethylsulfoxide/water around the phosphatidylcholine head group in solution](#)

The Journal of Chemical Physics **135**, 225105 (2011); <https://doi.org/10.1063/1.3658382>

# Comparative atomic-scale hydration of the ceramide and phosphocholine headgroup in solution and bilayer environments

Richard J. Gillams,<sup>1</sup> Christian D. Lorenz,<sup>2,a)</sup> and Sylvia E. McLain<sup>1,b)</sup>

<sup>1</sup>*Department of Biochemistry, University of Oxford, Oxford OX1 3QU, United Kingdom*

<sup>2</sup>*Department of Physics, King's College London, London WC2R 2LS, United Kingdom*

(Received 2 March 2016; accepted 12 May 2016; published online 8 June 2016)

Previous studies have used neutron diffraction to elucidate the hydration of the ceramide and the phosphatidylcholine headgroup in solution. These solution studies provide bond-length resolution information on the system, but are limited to liquid samples. The work presented here investigates how the hydration of ceramide and phosphatidylcholine headgroups in a solution compares with that found in a lipid bilayer. This work shows that the hydration patterns seen in the solution samples provide valuable insight into the preferential location of hydrating water molecules in the bilayer. There are certain subtle differences in the distribution, which result from a combination of the lipid conformation and the lipid-lipid interactions within the bilayer environment. The lipid-lipid interactions in the bilayer will be dependent on the composition of the bilayer, whereas the restricted exploration of conformational space is likely to be applicable in all membrane environments. The generalized description of hydration gathered from the neutron diffraction studies thus provides good initial estimation for the hydration pattern, but this can be further refined for specific systems. *Published by AIP Publishing.* [<http://dx.doi.org/10.1063/1.4952444>]

## I. INTRODUCTION

Lipid bilayers are an important component of any living system and have specifically evolved to maintain the contents of cells and organelles. Where once membranes of cells were thought to be a passive environment in which proteins resided and functioned,<sup>1</sup> in the last 20–30 years there has been a rapid expansion in the understanding of the range and complexity of the roles of lipid functionality in the membranes.<sup>2–5</sup> For example, lipids are essential in the regulation of blood vessel permeability,<sup>6</sup> blood clotting,<sup>7,8</sup> diabetic nephropathy,<sup>9</sup> and apoptosis.<sup>10</sup>

One particularly fascinating aspect of lipid behavior is the effect that hydration has on lipid function.<sup>11–13</sup> For instance, in the stratum corneum, it is important to regulate hydration such that the skin can act as an effective barrier.<sup>14–17</sup> The importance of hydration is highlighted by the fact that when cells become dehydrated, they modify their membrane composition to retain suitable fluidity.<sup>18,19</sup> Due to the partially hydrated nature of the bilayer headgroup region (existing between bulk water and the hydrophobic lipid tails) the lipid-lipid interactions in the headgroup region play a large role in determining the level of hydration that is experienced.<sup>20,21</sup> The hydration of the lipid headgroups in the membrane environment is therefore a complex interplay of the availability of the water, the way in which the lipids are packed into the bilayer and the affinity that each moiety of the headgroup has for interaction with water.

The phosphatidylcholine (PC) headgroup is one of the most common in human brain, umbilical cord endothelial

cells and indeed a large range of non-bacterial cells.<sup>22–24</sup> The sphingolipid ceramide is a major component of the skin<sup>25</sup> and is involved in many cellular processes, such as signalling,<sup>26</sup> and is implicated in membrane regulation through lipid flip flop.<sup>27</sup> Additionally, both of these lipids have been shown to act as biomarkers for Alzheimer's disease.<sup>28,29</sup>

In the current work, the levels of hydration and the location of the water in three-dimensional space around the headgroup within a bilayer has been assessed on the atomic length scale. Importantly, the hydration of specific headgroup moieties has been further compared to previous investigations on the atomic scale hydration of both ceramide<sup>30</sup> and phosphatidylcholine (PC) headgroup in solution.<sup>31–33</sup> These previous investigations have been benchmarked by experimental measurements outside the bilayer environment, as in solution—in the absence of aggregation—the local structure of lipid headgroup hydration is more easily accessible. The lipid-lipid interactions and the conformation of the lipid molecules in the bilayer are considered as a means for determining the driving forces for the difference in the hydration of the lipids in the bilayer compared with those in solution.

## II. METHODS

### A. Molecular dynamics simulations

A series of simulations were performed on five lipid bilayers containing different ratios of 1,2-dioleoylphosphatidylcholine (DOPC) and ceramide. Each contained a total of 200 lipids with molecular ratios of 99:1, 49:1, 19:1, 9:1, and 4:1 DOPC:ceramide. The lipids

<sup>a)</sup>chris.lorenz@kcl.ac.uk

<sup>b)</sup>sylvia.mclain@bioch.ox.ac.uk

were evenly distributed between the two leaflets of the bilayer, and no lipid flip-flop was observed on the time scale of this simulation. The simulations were carried out using the molecular dynamics (MD) simulation program LAMMPS.<sup>34</sup> CHARMM (C36) potentials<sup>35</sup> were used for the DOPC and a recent model,<sup>36</sup> based on CHARMM was used for the ceramide whilst water was modelled using the TIP3P parameters.<sup>37,38</sup> The analysis presented here focuses on the simulation of the bilayer containing 180 DOPC molecules and 20 ceramide molecules, whilst the remaining bilayers are used for analysis of the bulk properties. This lipid ratio was chosen to produce a liquid disordered bilayer, based on previous experimental work.<sup>39–41</sup> The bilayer was solvated with 9200 water molecules. The bond lengths and angles of the water molecules, as well as the hydrogen containing bonds in the lipid molecules were constrained using the SHAKE algorithm.<sup>42</sup> The system was equilibrated under NVE and NVT conditions prior to running under an NPT ensemble at 310.5 K and 1 atm for 100 ns. A time step of 2.0 fs was chosen, as is typical for an atomistic simulation using a velocity Verlet integrator. The van der Waals interactions were cut-off at 12 Å, with the energy and force smoothly ramped to zero between 10 Å and 12 Å. The PPPM algorithm<sup>43</sup> was used to compute the long-range Coulomb interactions. The final 90 ns of the simulations were used for analysis.

In order to put the current findings into context, the analysis of this work is compared with previous simulations from two recent papers. The hydration of the DOPC headgroup in solution has been investigated through the study of the lipid C<sub>3</sub>-PC dissolved in water<sup>31</sup> and the hydration of ceramide was investigated using a system containing ceramide, chloroform, and water.<sup>30</sup> In both cases the previous work was compared with experimental data, from neutron diffraction and NMR experiments. The excellent agreement with experimental data in both cases provides validation of the force fields used here for these molecules.

## B. ANGULA analysis

In order to assess the three-dimensional arrangements of molecules relative to one another, a program called ANGULA has been developed.<sup>44,45</sup> By assigning a set of orthogonal Cartesian axes to different parts of the molecules—in this instance the ceramide and DOPC headgroups and the water molecules—the location of neighboring molecules in 3-dimensional space relative to a particular moiety of a central molecule can be obtained. The resulting density of neighboring molecules can then be plotted as an isopycnic surface (connecting points of the same density) where this surface marks regions in space where the probability of finding neighboring molecules is above a certain threshold. The highest density of neighboring molecules is subsequently plotted<sup>46,47</sup> in the form of Spatial Density Maps (SDMs).<sup>48,49</sup>

In the work presented here, five coordinate systems were placed on each DOPC headgroup, three on each ceramide headgroup and one on each of the water molecules. These coordinate systems are used as a frame of reference to generate summed interaction patterns for the location of molecules around the defined groups on the lipids. The location of the coordinate systems is listed below and further details are provided in the supplementary material including a graphical representation of the location of the coordinate systems in Fig. S1 and S2.<sup>60</sup>

The labelling system used throughout this work is as follows:

- DOPC:
  - the “first ester” which is on the 1- position of the glycerol, furthest from the headgroup (on the right hand side of the DOPC molecule in Figure 1);
  - the “second ester”—the 2- position (on the left in Figure 1);
  - the phosphate group (PO<sub>4</sub><sup>−</sup>);
  - the CH<sub>2</sub> group next to the N1D nitrogen (C1D and two H0D);
  - the onium group (N(CH<sub>3</sub>)<sub>3</sub><sup>+</sup>).

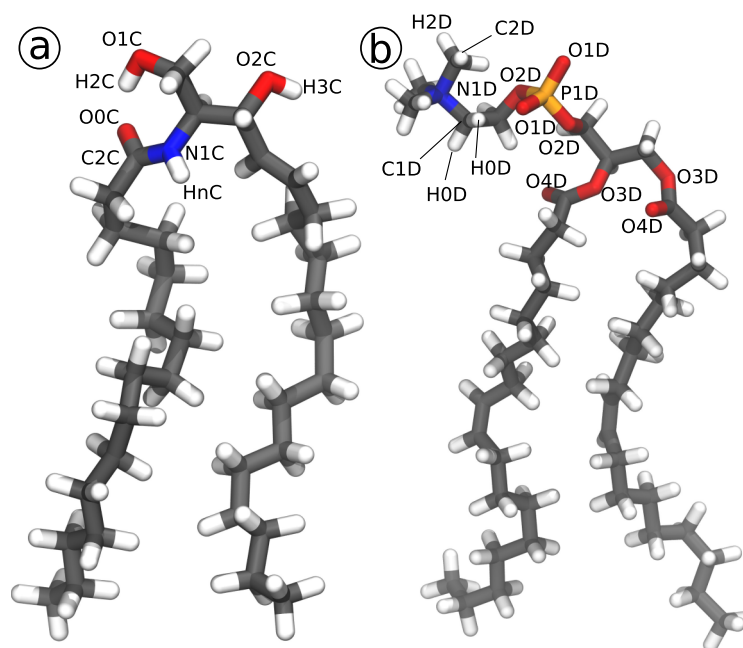


FIG. 1. The chemical structures of (a) ceramide and (b) DOPC, outlining the labelling scheme used to describe the different atoms throughout this text.

- Ceramide:
  - the amide group;
  - the “first hydroxyl” closest to the amide (O1C and H2C);
  - the “second hydroxyl” further from the amide (O2C and H3C).
- Water:
  - the central oxygen.

### III. RESULTS AND DISCUSSION

#### A. Area per lipid

The CHARMM (C36) force field provides a good representation of the area per lipid in a pure DOPC bilayer.<sup>35</sup> In addition the ceramide model used here was tested to ensure that the chain melting temperature and the area per lipid in the gel phase are in agreement with experimental measurements.<sup>36</sup> However, it is not clear whether this agreement would extend to a mixed lipid system. Ceramide has a propensity to condense bilayers and at high ceramide concentrations a gel phase would be observed at physiological temperatures. In order to assess whether there is a marked contraction in the bilayer, which would be concomitant with the formation of a gel phase, a number of methods are available to estimate the contribution of each lipid species to the cross-sectional area of the bilayer.<sup>50,51</sup>

Given that a set of bilayers with a range of concentrations of ceramide (1% to 20%) have been simulated, the partial specific area analysis proposed by Edholm and Nagle can be used (Fig. 2).<sup>52</sup> By considering the series of simulations, the contribution of each lipid species can be calculated through a linear regression analysis for the relationship between  $\text{Area}/N_{\text{DOPC}}$  and  $N_{\text{cer}}/N_{\text{DOPC}}$ , where  $N_{\text{DOPC}}$  and  $N_{\text{cer}}$  are the number of DOPC and ceramide molecules in the bilayer respectively. According to the equation

$$\frac{A(x)}{N_{\text{DOPC}}} = a_{\text{DOPC}}(x) + \frac{x}{1-x} a_{\text{cer}}(x), \quad (1)$$

where  $A(x)$  is the total area of the bilayer,  $x$  is the mole fraction of ceramide in the bilayer, and  $a_{\text{DOPC}}$  and  $a_{\text{cer}}$  are the area

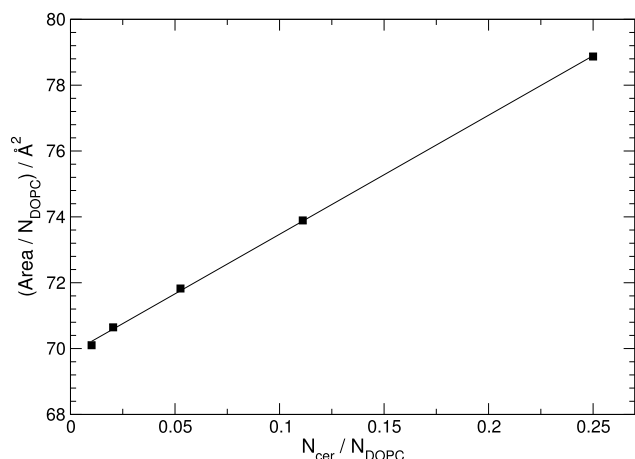


FIG. 2. The contribution of each lipid species in a bilayer can be estimated using the partial specific area analysis method proposed by Edholm and Nagle.<sup>52</sup>

per lipid contributions of DOPC and ceramide, respectively. The bilayer lies in the  $xy$  plane of the simulation box and so  $A(x)$  can be extracted from the average box lengths over the course of the simulation. The regression results in estimates of  $a_{\text{DOPC}} = 69.9 \text{ \AA}^2$  and  $a_{\text{cer}} = 36.2 \text{ \AA}^2$ . The straight line fit to the data with an  $R^2$  value of 1.00 indicates that these values provide a good estimate for the partial specific area across the range of ceramide concentrations considered here. There is no deviation from these values as would be expected were there to be the formation of a gel phase at higher ceramide concentrations.

In addition, a Voronoi analysis was performed using the VMD plugin, Memblugin,<sup>53</sup> on each of the simulation systems in isolation, giving a value for each system for both DOPC and ceramide. These values fall in the range of  $a_{\text{DOPC}} = 65.7\text{--}69.6 \text{ \AA}^2$  and  $a_{\text{cer}} = 52.7\text{--}54.7 \text{ \AA}^2$ . Although the Voronoi analysis gives a larger estimate for ceramide and a smaller estimate for DOPC—likely because the Voronoi analysis does not correct for the fact that the areas may impinge upon one another<sup>51</sup>—it shows that the area per lipid is consistent across the range of ceramide concentrations and thus confirms that all of the simulations are of fluid bilayer systems and there is no gel formation at high ceramide concentrations. See the supplementary material for further details and a graphical representation of the Voronoi data in Fig. S3.<sup>60</sup>

#### B. Lateral density profiles

The hydrophobic nature of the lipid bilayer interior results in a water concentration gradient across the lipid headgroup region, from a high concentration of water in the bulk liquid to a virtual absence of water in the acyl tail region. The hydration of any lipid headgroup moiety is therefore related to both the depth at which the headgroup is located within the bilayer as well as the affinity for the available water relative to the competing lipid-lipid interactions. Figure 3(a) shows the lateral density profile for the DOPC:ceramide bilayer simulation, with the density of lipid atoms plotted as a function of the distance (along the bilayer normal) from the bilayer center. Due to the low concentration of ceramide in the bilayer, the profile is plotted on a logarithmic scale to aid viewing (see Fig. S4 of the supplementary material for a plot on a linear scale).<sup>60</sup> As expected, the water density (cyan line; Fig. 3(a)) drops away rapidly from the bulk concentration outside the bilayer to approximately zero as the density of the lipid tails (DOPC-black and ceramide-purple) increases. The grey curves in Fig. 3 show the location of the DOPC headgroup - defined as all atoms above the ester group (including the carbonyl; see supplementary material for a full list of atom groupings).<sup>60</sup> It is clear that the DOPC headgroup is located further away from the bilayer center than the ceramide headgroup (magenta line). Although the water density begins to decrease in Fig. 3(a) as the lipid density starts to increase, the vast majority of the DOPC headgroup region is hydrated to some extent.

Given that the headgroup of ceramide is much smaller than that of DOPC, it is not surprising that the distributions do not cover as wide a range of  $z$ -values as the DOPC headgroup in Fig. 3(a). In order to gain more insight into

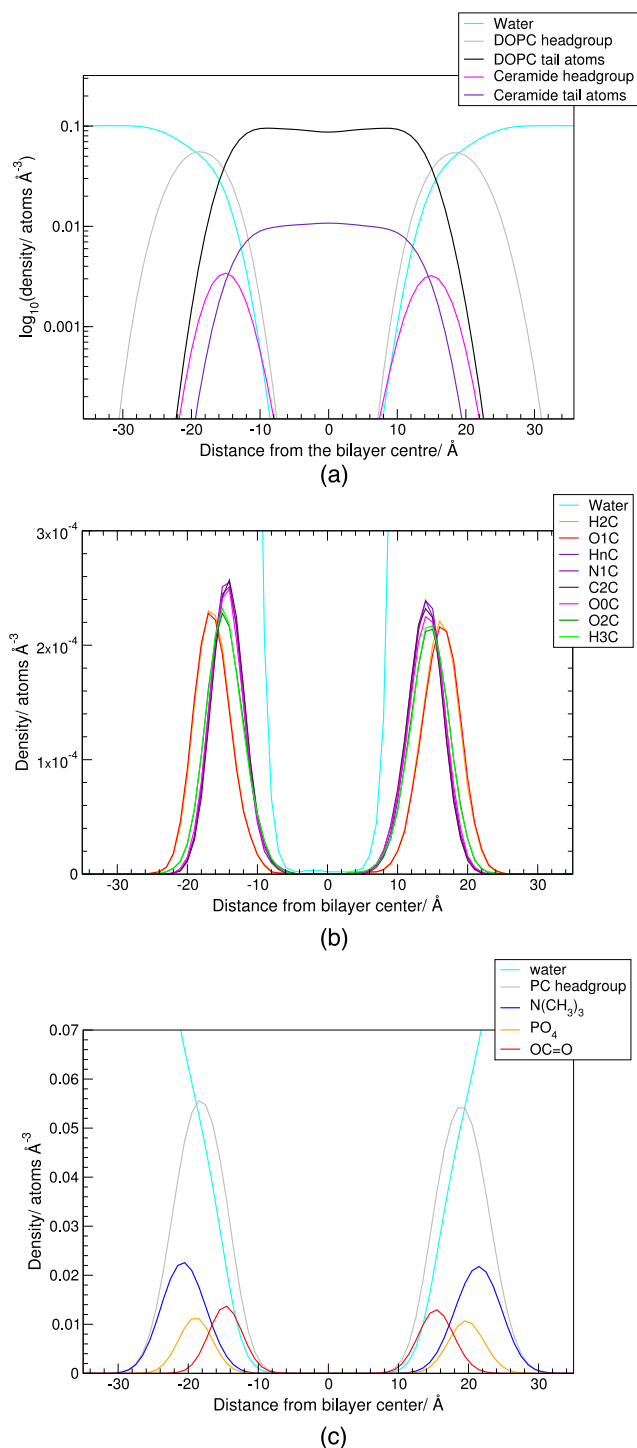


FIG. 3. Density profiles showing the distribution of different parts of the molecules along the  $z$ -coordinate (normal to the bilayer). DOPC is shown in grey and black and ceramide is shown in magenta and purple. (a) shows the density as a function of position in the  $z$  direction away from the center of the bilayer on a logarithmic scale to aid viewing, (b) shows the breakdown of the ceramide headgroup, and (c) shows a breakdown of the DOPC headgroup. (a)  $\log_{10}$  density profile. (b) Ceramide headgroup atoms. (c) DOPC headgroup moieties.

the hydration and location of the specific moieties of the ceramide molecule, the headgroup density peak can be split into its constituent atoms and this is shown in Fig. 3(b). It is interesting that the amide group atoms' distributions (HnC, N1C, C2C, and O2C—shown in purple/pink) are all in the

same  $z$ -range. This suggests that the plane of the amide group lies perpendicular to the  $z$  direction, i.e., the amide lies parallel to the plane of the membrane. This can also be seen by visual inspection of the simulation trajectory. The second hydroxyl group (O2C and H3C—shown in green) resides at a similar distance from the bilayer center to the amide group, whilst the first hydroxyl (O1C and H2C—shown in red/orange) sits closer to the bulk water.

Similarly, the DOPC headgroup is divided into the different functional groups in Fig. 3(c). If the headgroups of the DOPC molecules were completely extended it would be expected that the ester group (O3D and O4D—red) would be towards the inner edge of the grey distributions ( $\sim 10$ – $20$  Å), the phosphate oxygen atoms (orange) further away, and the onium group (blue) furthest from the bilayer center—at the outer edge of the grey distribution ( $\sim 20$ – $30$  Å). This is broadly what is observed in Fig. 3(c), except that rather than all of the onium density being located at the outer edge of distribution, it extends to overlap the phosphate and ester distributions. It has been previously shown that the phosphate and onium moieties of the phosphatidylcholine headgroup interact,<sup>20,21</sup> which leads to the onium group bending back away from the water interface, such that it would be found closer to the bilayer center than it would be were it to adopt a fully extended conformation. In terms of the hydration of DOPC, the water gradient across the headgroup means that there is more water available for the hydration of the onium group than the ester.

### C. Conformation of ceramide

When comparing the hydration between the solution and bilayer environments, a key factor is likely to be the molecular conformation of the lipids in question. In solution, the lipid tails are able to extend out in any direction, leading to the ceramide molecules adopting a range of conformations, with the tails close together or splayed apart. However, within a bilayer, the tails must remain close to one another, as they are confined to the hydrophobic acyl core. The site specific hydration will be dependent on the conformation as, in certain conformations, parts of the ceramide molecule will block the access of water to other regions of the headgroup—such as through the formation of an intra-headgroup hydrogen bond. In order to compare the conformation of the ceramide molecules, RDFs for intra-molecular headgroup interactions are shown in Figure 4 along with those from the previous investigation of ceramide in solution.<sup>30</sup>

The intramolecular RDFs show similar distributions of distances for both of the simulations, suggesting that the conformation of the ceramide headgroup does not dramatically change upon insertion into a bilayer. There are, however, some exceptions to this, most notably the HnC–O2C RDF (Fig. 1), where there is a greater proportion of large distances relative to ceramide in solution. In order to quantify the proportion of molecules in each conformation, coordination numbers are calculated by the integration of the RDFs via

$$n_{\alpha\beta}^B(r) = 4\pi \rho_{\alpha\beta} \int_{r_{\min}}^{r_{\max}} r^2 g_{\alpha\beta}(r) dr, \quad (2)$$



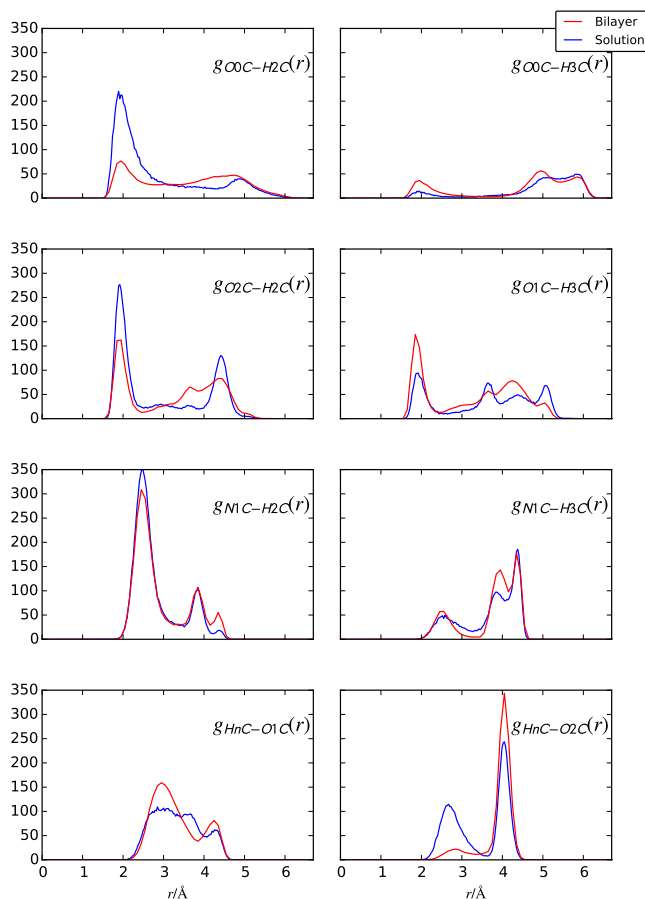


FIG. 4. Intramolecular RDFs showing the distribution of distances between different parts of the ceramide headgroup. The RDFs are shown for ceramide within a bilayer (red) and for ceramide dissolved in chloroform (blue).

such that a peak at higher  $r$  represents a more significant population than a similar sized peak at lower  $r$  values.

In solution, the number of molecules with HnC–O2C distances of  $\sim 2.5$  Å and  $\sim 4.0$  Å are relatively evenly populated (70% of molecules are at a distance greater than 3.45 Å), while in the bilayer the distribution is more distorted with 93% of molecules adopting the larger distance. Similarly, the OOC–H2C RDF also indicates a difference in headgroup conformation. In solution 63% of the molecules adopt a distance longer than 3.25 Å, which increases to 83% in the bilayer. In both environments more than half of the molecules adopt the conformation with the larger distance, but the distribution is more distorted in the bilayer, such that the shorter distances are much less common. These distance ranges can be used to investigate the effect of conformation upon hydration, by selecting subsets of ceramide molecules with intra-molecular distances of a certain length. An example of this analysis is shown in Fig. S5 of the supplementary material.<sup>60</sup>

In Section III B it was shown that the amide group was oriented parallel to the plane of the bilayer (the  $xy$  plane of the simulation box) and with the first hydroxyl group (OC1; Fig. 1) closer to the bulk water than the second (OC2). With this in mind, if both of the distances (HnC–O2C and OOC–H2C) observed in the intramolecular RDFs are shortened, the combination of these distances results in the

lipid tail being directed across the bilayer or towards the bulk water. The location of the unsaturated carbons (near to the second hydroxyl group) means that this directional preference would be propagated further down the chain, making it very unfavorable. This explains why these conformations are less likely to be found in the bilayer simulation.

#### D. Hydration of the ceramide headgroup

Due to its much smaller headgroup, ceramide (Figure 1) is significantly less soluble in water than DOPC and as a result it is not feasible to dissolve ceramide in water.<sup>54</sup> Therefore, the system that was used to investigate the hydration of ceramide in solution was a chloroform solution with a small amount of water ( $\sim 0.6$  water molecules per ceramide) added.<sup>30</sup> As a result, the density of water molecules in the bilayer and the solution systems is very different and the ceramide in the current bilayer study is significantly more hydrated compared with the previous investigation of hydration of ceramide in solution. The different water densities lead to different normalisation of the RDFs for water around the various atoms of the ceramide headgroup in Figure 5 and so it was necessary to scale down the solution RDFs by a factor of 40, in order to be able to compare them on the same axes. Despite the higher hydration in the bilayer systems, the RDFs are similar to those observed for the ceramide:chloroform:water

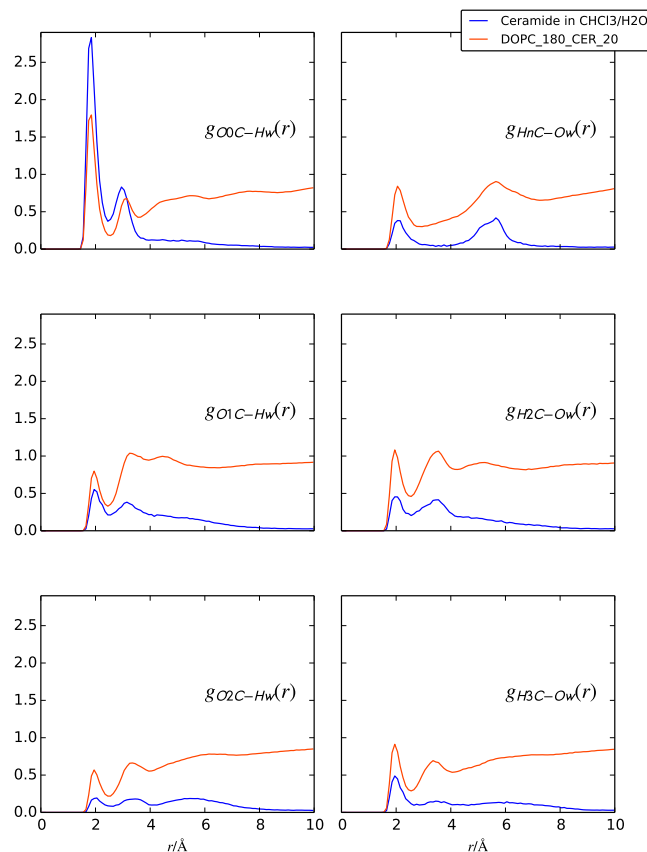


FIG. 5. RDFs showing the hydration of the ceramide headgroup in two environments: in chloroform and water (blue) and incorporated into a DOPC bilayer (red). The RDFs for the solution simulation have been scaled down by a factor of 40, so that they can be viewed on the same scale as the bilayer RDFs.

TABLE I. Coordination numbers for oxygen and hydrogen of water around different atoms of the ceramide headgroup. The distance at which the coordination number was calculated is listed in brackets and corresponds to the first minimum of each RDFs from Figure 5. The error estimates shown are based on the uncertainty in the value of  $r$  used to calculate the coordination number and do not reflect the uncertainty in the arrangement of atoms within the simulation box.

	cer/CHCl <sub>3</sub> /H <sub>2</sub> O	DOPC/cer bilayer
O0C-Hw	0.112 (2.45 Å)	$1.32 \pm 0.08$ (2.55 Å)
HnC-Ow	0.015 (2.95 Å)	$0.69 \pm 0.08$ (2.95 Å)
O1C-Hw	0.029 (2.45 Å)	$0.76 \pm 0.09$ (2.45 Å)
H2C-Ow	0.013 (2.45 Å)	$0.60 \pm 0.10$ (2.55 Å)
O2C-Hw	0.011 (2.45 Å)	$0.54 \pm 0.10$ (2.45 Å)
H3C-Ow	0.014 (2.65 Å)	$0.46 \pm 0.04$ (2.55 Å)

solutions. Not only are the peak positions similar for these RDFs but the hydration appears to be largely concentrated around the amide oxygen, with the first hydroxyl (O1C and H2C) experiencing higher levels of hydration compared with the second hydroxyl (O2C and H3C), with the trend in oxygen hydration matching that seen in solution—i.e., O0C > O1C > O2C. The trend of ceramide headgroup hydration is highlighted by the coordination numbers shown in Table I for ceramide in both the bilayer and in solution.

Due to the low ratio of water molecules to ceramide molecules in chloroform/water solutions, the coordination numbers are at least 10 times higher for the hydration of the bilayer. The trend of coordination across the three oxygen atoms is retained (O0C > O1C > O2C), but the increase in hydration in the bilayer relative to the solution is not uniform. For example, the carbonyl hydration is twelve times greater in the bilayer, but the second hydroxyl oxygen atom (O2C) and amide hydrogen atom (HnC) show close to a fifty fold increase in the coordination. This discrepancy is likely to be related to the increased intramolecular distance between the HnC of the amide and the second hydroxyl group (Fig. 4), which provides space for water molecules to interact.

The RDFs provide a convenient comparison between the two systems, but lack any three-dimensional information about the location of water molecules, for this purpose SDMs are shown in Figure 6. The SDMs are comprised of three components. Firstly, the segment of the molecule around which the coordinate system is defined is shown in the center of the map. The second feature is cross-sections of the density, through the origin, which are shown on the three panels around the back and below the map and thirdly, isopycnic surfaces containing the areas of highest density are shown. The color bar gives the density in atoms Å<sup>-3</sup> and applies to the panels and the isopycnic surfaces.

In agreement with the coordination numbers in Table I, the first hydroxyl group (O1C/H2C; Fig. 6(a)) shows a higher level of hydration compared with the second hydroxyl group (O2C/H3C; Fig. 6(b)). Similar to the ceramide headgroup in solution,<sup>30</sup> the water density is symmetrically distributed relative to the  $xy$ -plane in the SDMs with both regions of water density showing no preference for either the  $+y$  or  $-y$  direction. The hydration around the amide group in the bilayer in Fig. 6(c) shows a distribution of water which is

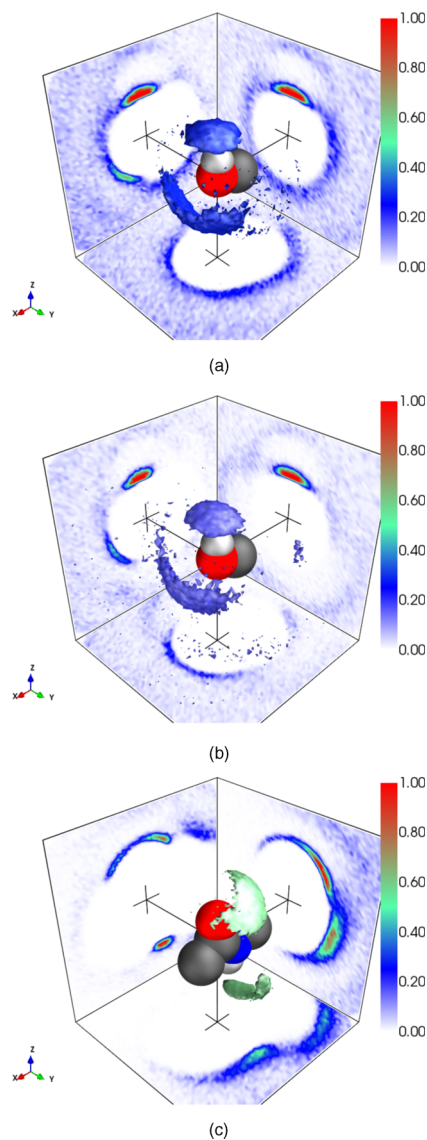


FIG. 6. SDMs for water around the ceramide headgroup in the bilayer, for the first (a) and second (b) hydroxyl groups and the amide group (c). The isopycnic surfaces contain 4% of water molecules in the regions with the highest density, within 8 Å of the central atom. (a) First hydroxyl hydration. (b) Second hydroxyl hydration. (c) Amide hydration.

asymmetric. Specifically, the hydration closest to the NH portion of the amide group shows a preference for hydration in the  $+y$  direction—most clearly seen in the cross sections on the back panel. Similarly, the hydration of the carbonyl oxygen is also asymmetric, where there is also a preference for this group to be hydrated in the  $+y$  direction, but in this case the hydration is also significantly skewed in the  $-x$  direction. In comparison to the ceramide in solution, where there was a symmetric density of water around the C=O group with relatively little NH hydration,<sup>30</sup> the 3-dimensional hydration of the amide group in the bilayer is highly asymmetric.

This dramatic shift in the water density surrounding the amide group for ceramide within a bilayer seems to be a result of the conformation of the ceramide headgroup, when it is confined to the lipid bilayer. Fig. 3(b) shows that the amide is restricted to lying parallel to the plane of the bilayer. This would result in one side of the amide group facing towards the acyl chain region of the bilayer and the other facing the bulk

water. Given the lack of water present in the acyl tail region, it is not surprising that this face of the amide is poorly hydrated compared to the face which is directed towards the water. This explains the distortion of the hydration to the  $+y$  direction in the SDM (Fig. 6(c)).

### E. Hydration of the phosphatidylcholine headgroup

There are a number sites on the PC headgroup where water molecules are likely to be located. Figure 7 shows the hydration RDFs for some of the salient headgroup atoms in accordance with the labelling scheme shown in Fig. 1. In this figure, the hydration in the DOPC:ceramide bilayer simulation

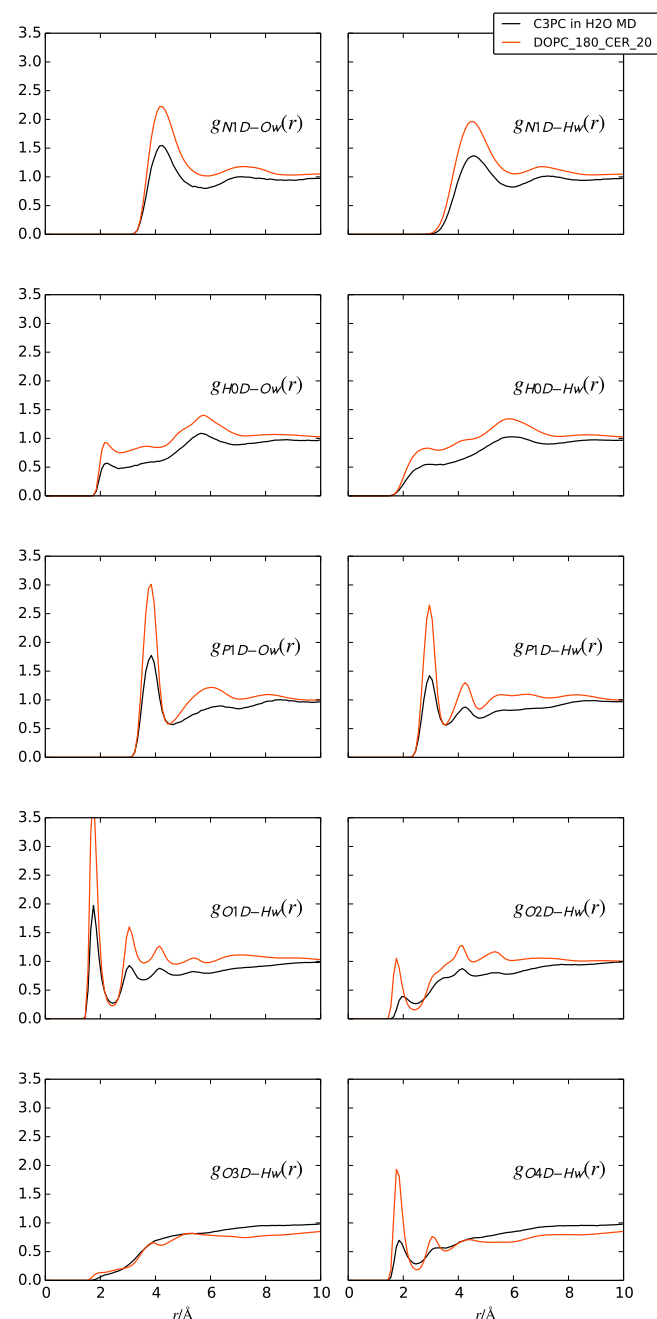


FIG. 7. RDFs showing the comparative hydration of the PC headgroup in two environments: in water solution (black),<sup>31</sup> in a bilayer in the presence of ceramide (red).

is compared with the results from previous MD simulations of C<sub>3</sub> PC in bulk water solvent.<sup>31</sup>

The hydration of the PC headgroup in both environments is similar, with the presence of peaks at the same positions in all of the RDFs in Fig. 7. Overall, the curves for the PC headgroup are higher in intensity, due (at least in part) to the excluded volume effect<sup>55</sup>—which is a result of local density at short distances being at variance with the bulk density—and from the fact that the atomic density is different for both systems. In order to make a more quantitative comparison of the PC headgroup hydration in these two different environments, the coordination numbers for the RDFs in Fig. 7 are listed in Table II. Again, the error estimates are based on the uncertainty in the distance at which the coordination number is calculated. In addition to the coordination numbers, the third column of the table shows the reduction in hydration for PC in the bilayer as a percentage of the hydration observed in the bulk solution—calculated by dividing the difference in coordination number by the coordination number for the solution.

In both the bilayer and solution systems, DOPC has large coordination numbers for the hydration of the nitrogen and phosphorus atoms which are at least partially due to the large distance ranges ( $\sim 6$  Å for N1D and  $\sim 3.5$  Å for P1D) over which these numbers are calculated. Water molecules are unlikely to interact directly with these two atoms in the PC headgroup, due to their crowded immediate environment, although the small peak in the H0D-Ow RDF indicates that there may be some direct interactions between water and the CH<sub>2</sub> group next to N1D. This behavior is similar to what has been reported for both PC in bulk solution<sup>31</sup> and for acetylcholine in solution.<sup>56</sup>

As opposed to previous work for the PC headgroup in aqueous solutions, within the bilayer, the headgroups are in much closer proximity to one another thus limiting solvent accessibility. Whilst the ceramide headgroup is confined to a relatively narrow range of  $z$ -values (Fig. 3(b)), the DOPC headgroup is spread over a larger distance and, as a result, experiences more marked differences in water density across the headgroup (Fig. 3(c)). The spread of the PC headgroup across the water gradient would be expected to lead to particularly significant reduced hydration in the bilayer environment for the ester groups.

TABLE II. Coordination numbers for water oxygen and hydrogen around the phosphatidylcholine headgroup. The distance at which the coordination number is listed in brackets and corresponds to the first minimum of each RDFs from Figure 7. The third column shows decrease in hydration seen in the bilayer relative to that in the solution.

	C <sub>3</sub> —PC/H <sub>2</sub> O	DOPC/cer bilayer	% red bil
N1D-Ow	21.16 (5.85 Å)	17.29 ± 1.54 (5.95 Å)	18%
H0D-Ow	0.77 (2.65 Å)	0.82 ± 0.13 (2.75 Å)	−5%
P1D-Hw	6.92 (3.55 Å)	6.01 ± 0.49 (3.55 Å)	13%
O1D-Hw	2.38 (2.45 Å)	2.11 ± 0.06 (2.45 Å)	11%
O2D-Hw	0.80 (2.45 Å)	0.72 ± 0.04 (2.45 Å)	10%
O3D-Hw	0.20 (2.45 Å)	0.20 ± 0.05 (2.45 Å)	−1%
O4D-Hw	1.25 (2.45 Å)	1.28 ± 0.08 (2.45 Å)	−3%



In order to compare the relative hydration levels of the different PC headgroup moieties, the third column of Table II shows the percentage by which the hydration in the bilayer is lower than that in the solution system. This comparison shows that the reduction is not uniform across all of the headgroup moieties, but interestingly it also shows that the relative decrease in hydration between the two systems is not solely determined by the distance from the bilayer center. For example, the N1D atom experiences a large decrease in hydration (18%) whilst the hydrogen atoms on the neighboring carbon atom do not show any significant loss of hydration—in fact there seems to be a small increase in hydration at this site. This may be related to the large distance range used for the coordination number of the N1D atom or it could indicate that the water around the H0D has a strong affinity for the H0D atoms, causing these water molecules to persist in the bilayer environment, which may in turn result from this CH<sub>2</sub> group being less involved in lipid-lipid interactions.

The trend in oxygen water coordination (O1D > O4D > O2D > O3D) is the same when the PC is in a bilayer or in solution, with the P=O (O1D) and C=O (O4D) oxygens showing the highest water coordination, whilst the P—O—C (O2D) oxygens show less hydration, and the C—O—C (O3D) oxygen atoms the least. The phosphate oxygen is ~10% less hydrated in the bilayer than in solution, whilst there is no significant change in the hydration of the ester oxygen atoms within the bilayer. The phosphate oxygens (O1D and O2D) show a comparatively high loss of hydration in the bilayer (Table II) even though this group is located further from the hydrophobic region of the bilayer than the ester oxygens (O3D and O4D), which experience no significant loss of hydration. This suggests that the dehydration of phosphate oxygens (O1D and O2D) must be related to their enhanced interaction with other lipid species as opposed to exclusion of water in this region—both the PID of the phosphate and its associated oxygen atoms (O1D and O2D) show roughly a 10% reduction in hydration. This, in conjunction with the comparative hydration of the N(CH<sub>3</sub>)<sub>3</sub><sup>+</sup> and its neighboring CH<sub>2</sub> group, suggests that lipid-lipid interactions may play a more significant role in the site specific reduction in hydration than the more general dehydration gradient (moving from bulk water to the acyl interior).

The spatial density maps (SDMs) for the hydration of DOPC headgroups within the bilayer are shown in Figures 8 and 9. The hydration of the terminal N(CH<sub>3</sub>)<sub>3</sub><sup>+</sup> group in Fig. 8(a) shows a distribution of water molecules which is very similar to the hydration of the PC headgroup in bulk solution.<sup>31</sup> The hydration pattern can be considered at three “levels” in the *z*-coordinate direction around the onium group. The first level is a region of hydration in the  $-z$  direction, with a patch of water below the three methyl groups. Moving towards the  $+z$  direction, there is a second level, where three regions of hydration are seen at a similar *z*-height to the methyl groups, where the density is located between the methyl groups. The third location of hydration is seen in the *z* direction at a height comparable to the carbon of the CH<sub>2</sub> group connected to the onium nitrogen. The clouds of density are closer to the nitrogen atom around the —CH<sub>2</sub> group, as can be seen in the cross-section on back right hand

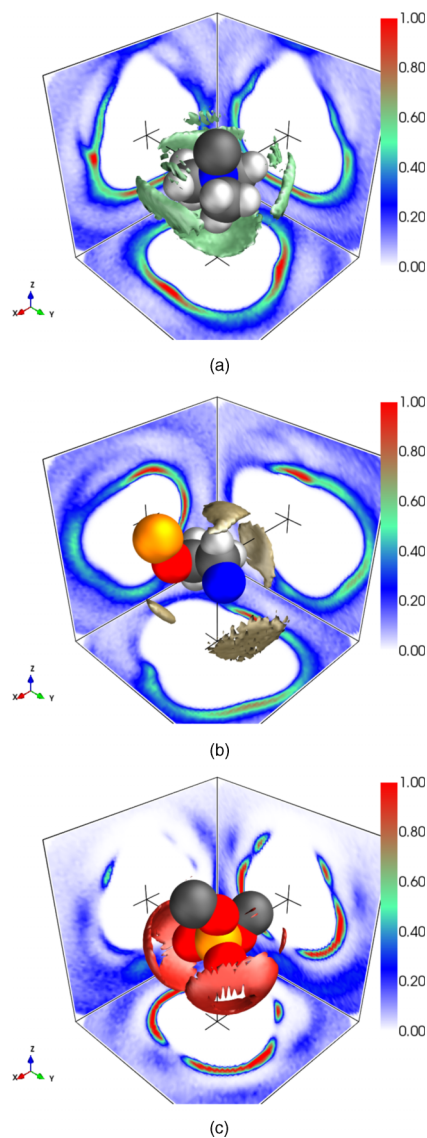


FIG. 8. SDMs for water around the DOPC headgroup, showing (a) N(CH<sub>3</sub>)<sub>3</sub><sup>+</sup> group, (b) the CH<sub>2</sub> group next to N1D, and (c) the PO<sub>4</sub><sup>−</sup> group. The SDMs are shown at an isocontour level of 4% of the water molecules within 8 Å of the central atom, with the exception of the phosphate group which shows 7% of water molecules. (a) [N(CH<sub>3</sub>)<sub>3</sub>]<sup>+</sup> hydration. (b) H0D hydration. (c) [PO<sub>4</sub>]<sup>−</sup> hydration.

panel. The first and second levels of hydration between the CH<sub>3</sub> groups are somewhat intuitive, with the water molecules approaching through the gaps in the methyl groups towards the nitrogen atom, but it is not clear why there would be three distinct regions of hydration in this third ‘level’. Consistent with the H0D-Ow RDF in Fig. 7, this arrangement of water density suggests that water molecules are tucked between the nitrogen atom and the choline carbon atoms, similar to the hydration of the PC headgroup in bulk solution.<sup>31</sup> Neutron diffraction measurements of the amino acid glutamine in solution also indicate some hydration of CH groups in close proximity to the terminal NH<sub>3</sub><sup>+</sup> group in aqueous solutions.<sup>57</sup>

It should be noted that in the SDMs the location of the isopycnic surfaces is only defined relative to the atoms used to define the coordinate system. Beyond these atoms, the surfaces will show an average location based on the range of

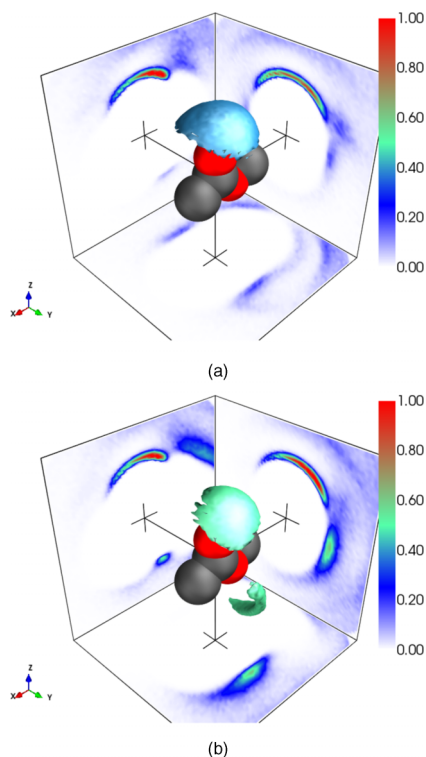


FIG. 9. SDMs for water around the ester groups of DOPC, showing (a) the first ester group hydration (left-hand tail in Fig. 1) and (b) second ester group hydration (right-hand tail in Fig. 1). The SDMs are shown at an isocontour level of 5% for all molecules within 0–8 Å of the central atom. (a) First ester hydration. (b) Second ester hydration.

conformations that the molecules adopt in the simulation. The coordinate system specified for the  $\text{N}(\text{CH}_3)_3^+$  SDM (Fig. 8(a)) holds the central nitrogen and the bonded carbon atoms in place but the  $\text{CH}_2$  is free to rotate relative to the axis system (i.e., the hydrogens can adopt any position around the carbon) and so the density observed in the third level around this group is in fact an average of the water locations across a range of conformations around the  $\text{CH}_2$  group. If the  $\text{CH}_2$  group underwent completely free rotation, with no preferred conformation, then this density would be averaged into a ring of density. The presence of three discrete regions of hydration indicates that the hydrogen atoms do not randomly sample all different conformations, but instead are more likely to be located above the gaps between the methyl groups. In order to verify this observation, the frame of reference can be moved onto the  $\text{CH}_2$  group. This allows a SDM to be plotted with the  $\text{CH}_2$  carbon at the center and the hydrogen atoms integrated into the coordinate system, such that their conformation is fixed (Fig. 8(b)). It is clear from this figure that the water molecules are directly approaching the hydrogen atoms of the  $\text{CH}_2$  group as there is density directly above hydrogen in the  $+z$  direction as well as above the hydrogen in the  $-x$  direction. The other patch of hydration in the  $+x$  direction appears to be related to water coordination to the  $\text{P}=\text{O}$  oxygen.

The preference for water around the  $\text{PO}_4$  group is also seen in the phosphate-water SDM (Figure 8(c)) with density caps around the  $\text{P}=\text{O}$  (O1D) atoms. Further, there are some smaller patches of water density around the  $\text{P}-$

$\text{O}-\text{C}$  O2D atoms. Similar to the PC headgroup in bulk solution,<sup>31</sup> the hydration pattern for the phosphate group is symmetric, indicating that the phosphate portion of the DOPC headgroup is not oriented across the water concentration gradient.

Figures 9(a) and 9(b) show the SDMs for both ester groups from the glycerol tail linkages for DOPC. Specifically, Fig. 9(a) shows the ester on the 1-position of the glycerol and Fig. 9(b) shows the ester in the 2-position of the glycerol. In both of these SDMs there is a significant amount of density in the  $+z$  direction directly above the carbonyl oxygen atoms (O4D). In both cases this density is distorted towards the  $\text{C}-\text{O}-\text{C}$  oxygens (O3D) in the  $-x$  direction. In addition, both of the ester groups show hydration below (in the  $-z$  direction) the O4D ( $\text{C}-\text{O}-\text{C}$ ) oxygen—which can be seen on the left hand panel of the figure. However, there is a marked difference between the two esters. Firstly, the patch of hydration below O4D in the second ester is much more pronounced and secondly the density of water around both the O3D and O4D oxygen atoms is severely distorted in the  $+y$  direction for the second ester.

The position of the ester groups on the central glycerol backbone (occupying the 1- or 2-position) alters the hydration of these groups. It appears that there are two effects which combine to alter the hydration of one relative to the other. Firstly the second ester is slightly closer to the lipid phosphate group and as such is closer to the bulk water solvent. The second aspect is similar to the behavior seen for the amide group in ceramide, where one side of the moiety faces towards the bulk water solvent and the other towards the acyl chain region. Being closer to the rest of the headgroup gives the second ester less flexibility to orient above the acyl chain region of the tail. As a result, the ester group can become restricted to lying parallel to the plane of the bilayer, as there are limitations to the torsional degrees of freedom between the glycerol backbone and the acyl tail. The first hydroxyl group has additional freedom and is further from the phosphate and onium groups and therefore can adopt a wide range of angles relative to the bilayer, resulting in a less distorted hydration pattern.

In addition to the SDMs, the orientation of water molecules around the DOPC headgroup has been determined. Figure 10 shows the distribution of two angles  $\phi_1$  and  $\phi_2$ . These angles describe how a water molecule approaches a selected atom in the lipid and the angles are defined such that if  $\phi_1$  is less than  $90^\circ$  the hydrogen atom side of water is directed towards the atom in question whilst a  $\phi_1$  angle greater than  $90^\circ$  then the oxygen is closer to the atom in question. The second angle  $\phi_2$  defines the tilt of the water molecule using the angle between two vectors, the first is from the solvated atom to the oxygen of water and the second is between the two hydrogen atoms of the water molecule. The supplementary material defines both  $\phi_1$  and  $\phi_2$  graphically in Fig. S6.<sup>60</sup>

The distribution of angles seen here for water approaching the nitrogen and phosphorus of DOPC are very similar to the hydration of the PC in aqueous solution.<sup>31</sup> The  $\phi_1$  angle for

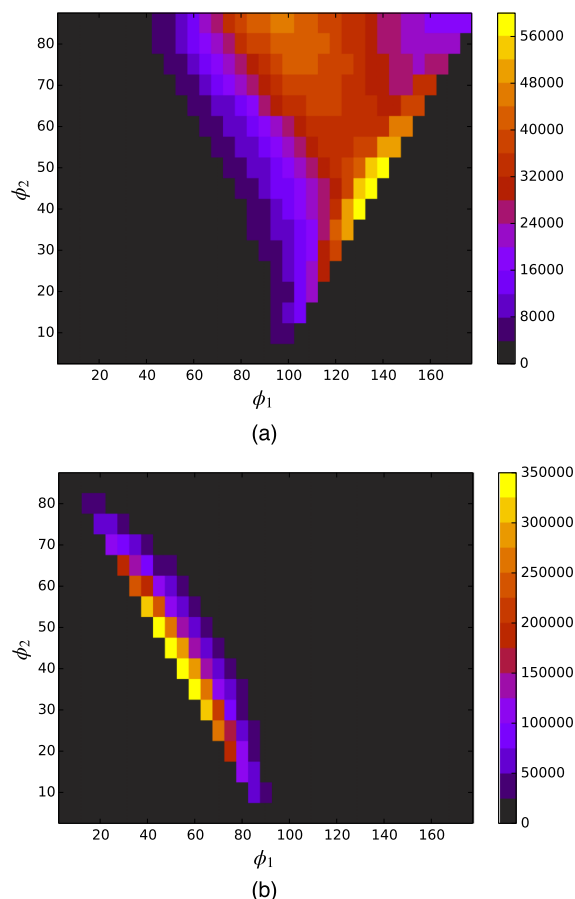


FIG. 10. The distribution of  $\phi_1$  and  $\phi_2$  angles for water approaching the nitrogen and phosphorus atom of the phosphatidylcholine headgroup. (a) Water orientation around  $\text{N}(\text{CH}_3)_3^+$ . (b) Water orientation around  $\text{PO}_4^-$ .

the nitrogen is distributed around angles of  $\sim 140^\circ$ , indicating that the oxygen atom is approaching the  $\text{N}(\text{CH}_3)_3^+$  group, while around the phosphate group the  $\phi_1$  angle is centered around  $\sim 50^\circ$  indicating that the hydrogen atom of the water is directed towards the  $\text{PO}_4^-$  group. In addition, the water interacting with the  $\text{PO}_4^-$  group shows a much narrower distribution of  $\phi_2$  angles due to hydrogen bonding from the surrounding water molecules to the  $\text{P}=\text{O}$  oxygens showing that  $\text{O}\cdots\text{H}-\text{O}$  angle is nearly linear, showing restricted range of hydrogen bonding angles. For the water molecules around the  $\text{N}(\text{CH}_3)_3^+$  group on the other hand, the  $\phi_2$  distribution is fairly broad indicating that water coordination around this portion of the PC headgroup is driven by electrostatics rather than by direct hydrogen bonding interactions.

## F. DOPC-DOPC interactions

Due to the abundance of DOPC in the bilayer simulated here, the majority of the headgroup interactions occur between DOPC molecules. While there are clearly many possible interactions which could occur between these lipids, only the interactions which show the highest densities are shown by way of SDMs in Figure 11. The supplementary material provides a more comprehensive set of DOPC-DOPC headgroup interactions in Fig. S7.

Figs. 11(a) and 11(b) show the first and second ester group interactions with the onium headgroup of other DOPC molecules. Interestingly, the second ester group has more pronounced interactions with neighboring DOPC  $\text{N}(\text{CH}_3)_3^+$  groups compared with the first ester group, despite their identical chemical structure. Both ester groups contain an area of density above the carbonyl oxygen atom and displaced in the  $-x$  direction. However, the second ester interactions are more

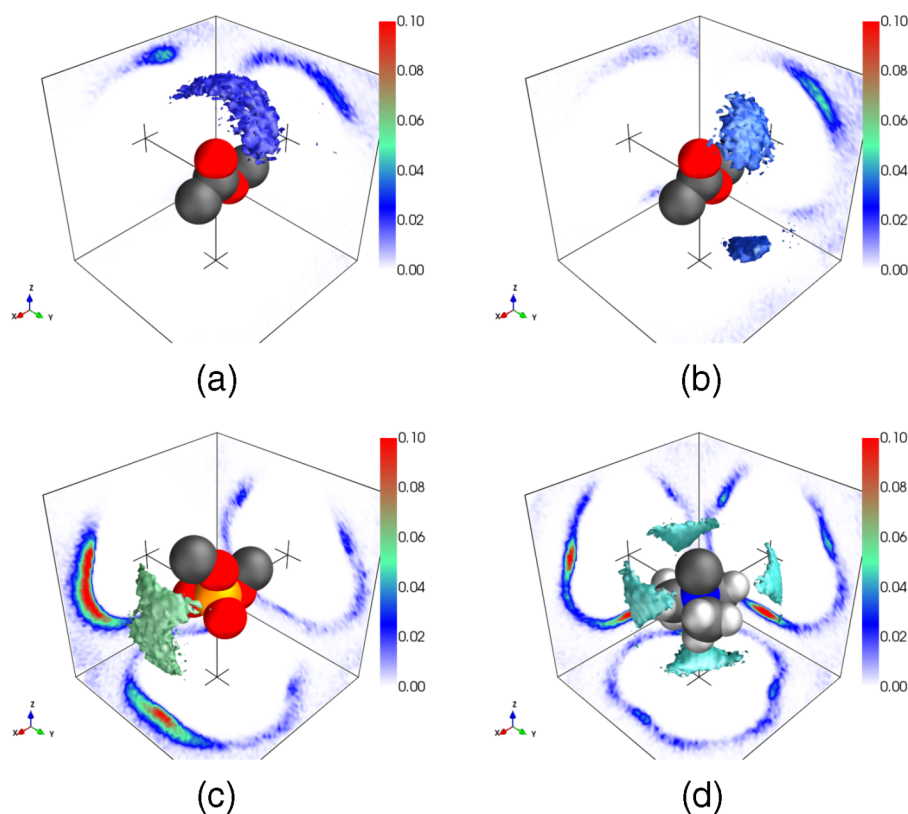


FIG. 11. DOPC-DOPC SDMs showing the location of the DOPC nitrogen around the first (a) and second (b) ester groups and around the  $\text{PO}_4^-$  group (c). (d) shows the inverse of plot (c), i.e., location of phosphate P atoms around the  $\text{N}(\text{CH}_3)_3^+$  group. The SDMs are shown at an isocontour level of 9% of the DOPC molecules within  $8 \text{ \AA}$  of the central atom. (a) 1<sup>st</sup> ester- $\text{N}(\text{CH}_3)_3^+$ . (b) 2<sup>nd</sup> ester- $\text{N}(\text{CH}_3)_3^+$ . (c)  $\text{PO}_4^-$ - $\text{N}(\text{CH}_3)_3^+$ . (d)  $\text{N}(\text{CH}_3)_3^+$  -  $\text{PO}_4^-$ .



localized with most of the density located in the  $+y$  direction and a further band of density located below ( $-z$  direction) the C—O—C linkage. The second ester group Fig. 11(b) is situated further from the bilayer center and closer to the  $\text{N}(\text{CH}_3)_3^+$  group, which explains the higher density of both onium contacts and hydration (Fig. 9) around this. In addition, this second ester group has a restricted orientation, due to its proximity to the  $\text{PO}_4^-$  moiety and as such the  $\text{N}(\text{CH}_3)_3^+$  density is significantly more distorted in the  $+y$  direction, as one side of these groups is facing towards water layer. The ester- $\text{N}(\text{CH}_3)_3^+$  group interactions suggest that water is displaced when there is lipid-lipid association around either of these groups as the SDMs for the hydration of both the ester groups in Fig. 9 and in Figs. 11(a) and 11(b), show density shells in similar locations.

Compared with the ester group contacts, the  $\text{N}(\text{CH}_3)_3^+ - \text{PO}_4^-$  contacts are more pronounced in the SDMs in Figs. 11(c) and 11(d), where these two figures are the inverse of one another with Fig. 11(c) showing preferential locations of the onium group around the  $\text{PO}_4^-$  regions of the PC headgroup and Fig. 11(d) showing the preferential locations of  $\text{PO}_4^-$  around the  $\text{N}(\text{CH}_3)_3^+$  motifs. It is worth noting that, in Fig. 11(c), the carbon in the  $+z$  and  $+x$  direction is that of the glycerol backbone and the carbon on the  $-x$  side is that of the choline headgroup. Interestingly, the  $\text{N}(\text{CH}_3)_3^+$  density is largely contained between the two P=O atoms, in a tight band. This is in stark contrast to the hydration of the phosphate group (Fig. 8(c)), which shows caps of hydration around the oxygen atoms. The location of the  $\text{PO}_4^-$  group around the  $\text{N}(\text{CH}_3)_3^+$  group (Fig. 8(d)) shows that the association between these two groups is near the N atom between the methyl groups, similar to the water hydration of  $\text{N}(\text{CH}_3)_3^+$  seen in Fig. 8(a). Combining the information from both Figs. 11(c) and 11(d), it is likely that this close interaction stems from the headgroup of the DOPC being in a bent configuration, such that the  $\text{N}(\text{CH}_3)_3^+$  group is at a similar distance from the bilayer center to the  $\text{PO}_4^-$  group. In the lateral density profile for the different aspects of the DOPC (Fig. 3(c)) there is significant overlap between these two groups, however there is also a significant portion of the  $\text{N}(\text{CH}_3)_3^+$  group further from the bilayer center than the  $\text{PO}_4^-$  group. The  $\text{N}(\text{CH}_3)_3^+$  group is a bulky group, so it is conceivable that part of that group is tucked down next to a neighboring  $\text{PO}_4^-$  group and the remainder of the  $\text{N}(\text{CH}_3)_3^+$  has a greater number of contacts with water.

Whilst there are similarities between the SDMs for the hydration (Fig. 8(a)) and the location of the phosphate group (Fig. 11(d)) around the onium moiety, there are also differences. The  $\text{PO}_4^-$  coordination to the  $\text{N}(\text{CH}_3)_3^+$  at the  $-z$  level remains similar to the hydration around this group, with a region of density in the gap between the three methyl groups. The second level of water coordination at a similar  $z$  height to the central nitrogen atom is absent for the phosphate group and instead the third level of coordination (at higher  $z$  values) is more marked compared with the hydration seen in Fig. 8(a). This is likely a result of steric hinderance as the  $\text{PO}_4^-$  group being too large to fit in the small gaps between two methyl groups and instead approaches into the regions between three methyl groups (directly opposite

the position of the N—C bond on the other side of the nitrogen).

## G. Ceramide-ceramide interactions

The ceramide-ceramide interactions are less pronounced than the DOPC-DOPC, due to the small amount of ceramide in the bilayer (10%), which is reflected in the scale bar of the SDMs. The ceramide molecules do not appreciably aggregate throughout the course of the simulation (see Fig. S8 of the supplementary material for a contact analysis).<sup>60</sup> The three sites on the headgroup described in Sec. II were used for ANGULA analysis, giving nine interaction pairs for SDM analysis, however the most significant interactions involve the amide group and specifically the amide group interaction with the second hydroxyl produces a particularly high density on the SDM. As a result the location of the three parts of the ceramide headgroup around the amide group of neighboring ceramide molecules is shown in Figure 12, alongside the inverse figure showing the location of the amide group around the second hydroxyl group. The full set of nine SDMs is included in Fig. S9 of the supplementary material.<sup>60</sup>

The SDMs in Fig. 12 show the most prominent ceramide-ceramide interactions, which are between the second hydroxyl group—the hydroxyl group furthest away from the amide bond (Fig. 1) and the amide group on neighboring ceramide molecules. The lateral density profile for parts of the ceramide headgroup (Fig. 3(b)) shows that the first hydroxyl sits in a different plane to the amide and the second hydroxyl, which are located closer to the center of the bilayer resulting from the constraint imposed upon the conformation of the ceramide headgroup upon inclusion in the bilayer. In order for the acyl tails to remain in the bilayer center, the conformation of the headgroup becomes locked with the amide lying parallel to the plane of the membrane. Although the conformation between the amide and the second hydroxyl is constrained, the C—O bond of the hydroxyl is free to rotate, and the more extended conformation of the headgroup means that the amide can be approached from any side. As a result, it is unsurprising that the distribution of the second hydroxyl group is similar to the hydration pattern of the amide in the liquid simulation. It does not contain the same  $+y$  distortion seen in the hydration of the bilayer system, because the hydroxyl group is restricted to the plane of the amide group. The density profiles (Fig. 3(b)) showed that the first hydroxyl group sits closer to the water environment than the amide and the second hydroxyl moiety, which are in the same plane as one another. As a result, the coordination numbers for the hydration of the first hydroxyl group are larger (see Table I) and the intermolecular interactions of ceramide are dominated by the amide group and the second hydroxyl group, with the first hydroxyl group preferentially interacting with the water.

## H. DOPC-ceramide interactions

The interactions of ceramide and DOPC show examples of the behavior that governed the hydration of these headgroups (Sections III C and III D). For example, there is very little



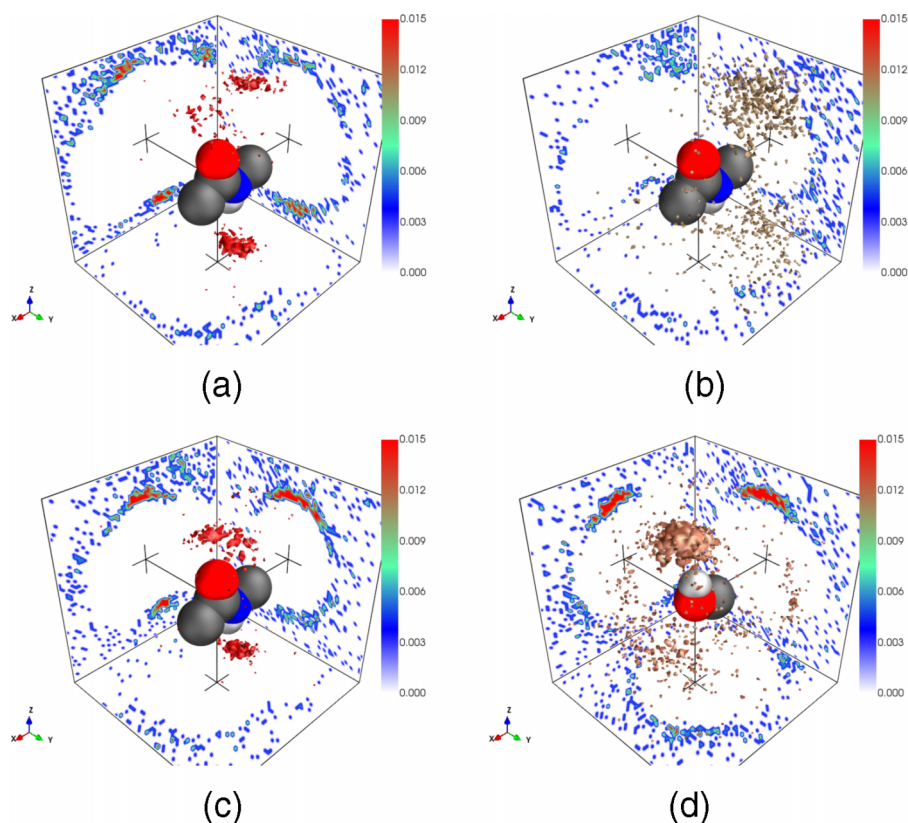


FIG. 12. Ceramide-ceramide interactions. These SDM show interaction on the amide group. Namely, the location of amide carbon atoms around the amide group (a), the first hydroxyl oxygen around the amide (b), the second hydroxyl oxygen around the amide (c) and the amide around the second hydroxyl (d). The density is plotted for molecules within 8 Å of the central atom and the percentage of molecules enclosed in the isopycnic surface is shown in brackets in the labels above. (a) Amide - Amide (8%). (b) Amide—1<sup>st</sup> OH (14%). (c) Amide—2<sup>nd</sup> OH (7%). (d) 2<sup>nd</sup> OH—Amide (7%).

density of ceramide headgroup around the phosphate and onium groups, due to the ceramide position being lower in the bilayer. This density is greater for the first hydroxyl group which sits closer to the position of the phosphate and onium groups. This behavior is also seen in the location of the DOPC moieties around the regions of ceramide, with the phosphate group producing the highest density around the first hydroxyl group of ceramide, whilst the ester groups show the highest density around the amide and second hydroxyl group. Similarly the amide group of the ceramide molecule shows a distorted distribution of onium and phosphate groups, with the density located on the same side of the amide group as the water as is seen in Figs. 13(a) and 13(b). Given that the phosphate and onium groups are located closer to the bulk water than to the acyl chain, this distortion is unsurprising. The ester groups do not show the same distortions as the amide (Figures 13(c) and 13(d)). Moreover, the distributions of the ceramide amide around the ester groups of DOPC are not identical, with the first ester showing more density on the sides (out of the  $xz$ -plane), whilst the second ester amide distribution is more restricted to being in the plane of the ester group. This is consistent with the amide group being confined to laying parallel with the plane of the bilayer and the amide groups being found at a similar height in the bilayer to the ester groups. See the supplementary material (Figs. S10 and S11)<sup>60</sup> for a full set of interaction SDMs for both ceramide moieties around DOPC and for DOPC around ceramide.

### I. Lipid conformation

In addition to the position of the different functional groups, the work presented here describes constraints on the

conformation of the headgroups as a result of the lipid tails being confined to the hydrophobic bilayer interior. This limits the freedom of rotation in the region at the top of the lipid tails and across the bridging group between the two tails (the amino alcohol of the ceramide and the glycerol region of the DOPC). An example of a typical conformation of the ceramide headgroup and the DOPC headgroup is shown in Figure 14.

In Fig. 14, the ceramide is oriented such that the plane of the amide group is parallel to the plane of the membrane (the  $xy$ -plane of the simulation box). Comparing the amide group in Fig. 14 to the representation in amide hydration SDM (Fig. 6(c)), the  $z$ -axis for the SDM would be pointing into the page in Fig. 14 (along the C=O bond) and the  $x$ -axis would be pointing from left to right. This means that the  $+y$  direction, where the increased hydration was observed in Fig. 6(c), would be above the amide, where the bulk of the water molecules are located in Fig. 14. Similarly, the  $\text{PO}_4^-$  and  $\text{N}(\text{CH}_3)_3^+$  groups are seen in the same region of the SDMs for DOPC around ceramide (Figs. 13(a) and 13(b)), as they are found further towards the bulk water than the amide group (Fig. 3).

The DOPC conformation is less directly constrained, but again the configuration leads to distortions in the density of surrounding water and lipid molecules around the two ester groups. In Fig. 14, the left hand tail is on the 1-position of the glycerol backbone with the first ester further from the headgroup compared with the second ester on the 2-position. This seems to restrict the conformations adopted by the second ester and it leads to there being one face of the ester looking towards the bulk water, which is evidenced by the distorted shape of the cloud of water density below the

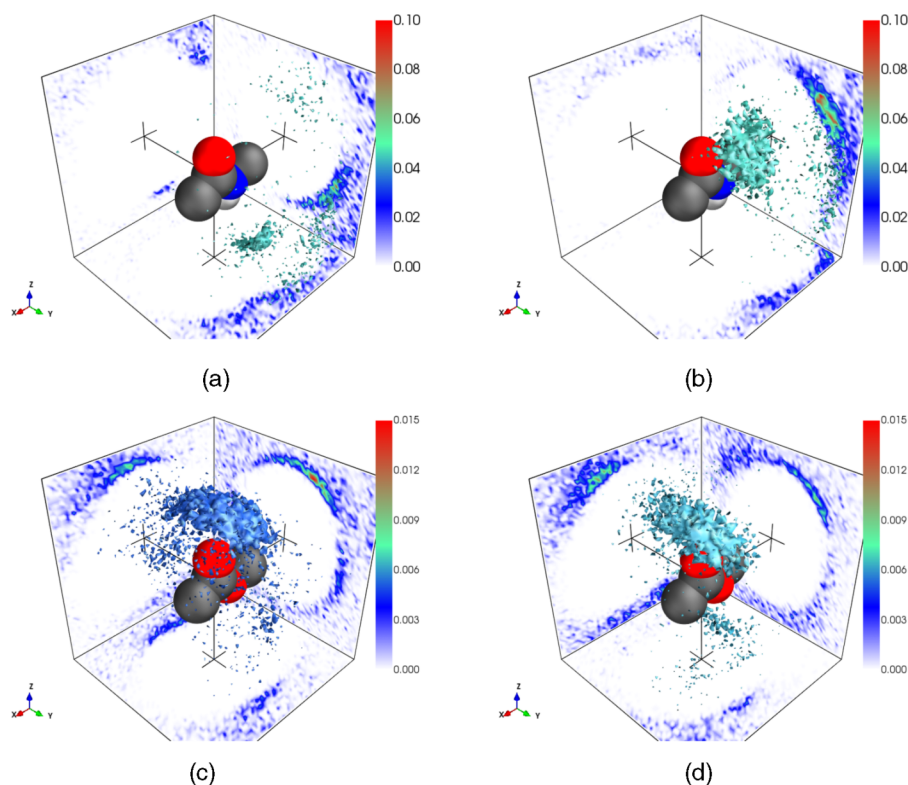


FIG. 13. SDMs for interactions between DOPC and ceramide. The top row concerns the distribution of DOPC around the ceramide headgroup—(a) shows the DOPC phosphate group and (b) the onium group around the ceramide amide. The bottom row shows ceramide around DOPC, namely the ceramide amide around the first ester (c) and second ester (d) of DOPC. A percentage (given in brackets) of the surrounding molecules within 8 Å of the central atom are enclosed in the isopycnic surfaces. (a) Amide— $\text{PO}_4^-$  (5%). (b) Amide— $\text{N}(\text{CH}_3)_3^+$  (9%). (c) 1<sup>st</sup> ester—Amide (7%). (d) 2<sup>nd</sup> ester—Amide (6%).

O4D oxygen position in Fig. 9(b). Again comparison of the orientation of the second ester group in Fig. 14 with the SDM for that moiety reveals that it is indeed the side facing the bulk water which is more hydrated. The first ester group, being further from the headgroup, has enough conformational freedom to enable a more symmetric distribution of water. The first ester group seems to sit slightly lower in the membrane, further from the bulk water which would explain the decreased interaction with water and increased interaction with ceramide relative to the second hydroxyl group.

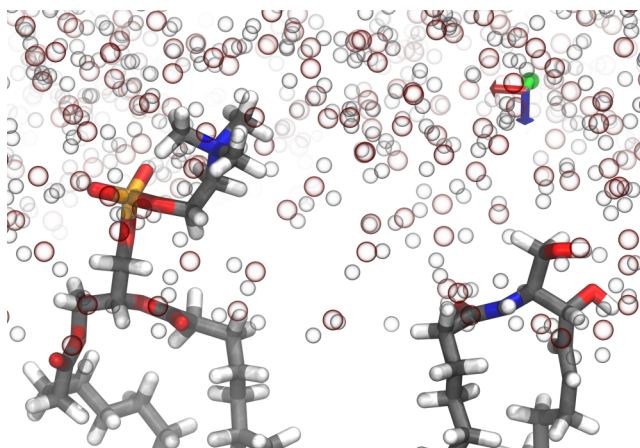


FIG. 14. Typical conformation of the lipid headgroups when in the bilayer. DOPC is shown on the left and ceramide on the right hand side of the figure. The bulk water sits above the headgroups and the hydrophobic interior of the bilayer at the bottom of this figure. Only two of the lipids from the bilayer and a subset of the water molecules have been shown for the benefit of clarity.

#### IV. CONCLUSIONS

The interaction of the lipid headgroups within the bilayer leads to a complex environment in which the hydration of the lipids is affected by the height of the different moieties within the bilayer, the conformation of the lipid molecules, and the interplay of the affinities for lipid-lipid and lipid-water interactions. Generally speaking, for the solvent accessible portions of the lipid headgroups, the lipid-lipid interactions are in direct competition with the hydration of the lipids, with the same regions of the headgroup showing similar coordination. The exception to this is the DOPC  $\text{PO}_4^-$  group, where the dominant lipid-lipid interaction (with the onium group) occurs at a different location than the hydration interactions. However, this does not seem to prevent the phosphate group from being somewhat dehydrated in the bilayer environment relative to the solution simulation (Table II). The onium and phosphate groups are both large and as a result, the bulk of the onium group seems to restrict the access of water, even though the site of interaction is different from the site of hydration. This is highlighted in Table II, which shows that both the phosphate and onium groups experience significantly less hydration in the bilayer environment.

The ester groups of DOPC retain similar hydration to that seen for the  $\text{C}_3\text{PC}$  solution,<sup>31</sup> i.e., there is no reduction in hydration upon insertion into the bilayer, and are consistent with previous investigations.<sup>58,59</sup> However, the two esters show different hydration and lipid-lipid interactions from one another, due to the different orientation and depth of these ester groups within the lipid bilayer. The regions of interaction around the second ester differ, depending on the neighboring moiety in question. In the case of moieties found further

from the bilayer center, such as the phosphate, the onium, and water, the interactions are distorted in the  $+y$  direction. However, the moieties which are found at a similar height in the bilayer, such as the ceramide headgroup, do not show the same level of distortion. It should be noted here that in the previous MD simulations C=O groups were slightly undersaturated compared with neutron diffraction data, due to slight aggregation of the lipids in solution.

The hydration of both the ceramide –OH groups shows good agreement with the preferred hydration observed in solution,<sup>30</sup> with both systems showing less hydration around the oxygen atom of the second hydroxyl in comparison to the first hydroxyl. However, the amide group shows differing patterns of hydration in the two environments. In the solution system, the most hydrated regions were located around the plane of the amide group, but in the bilayer system these regions experience a large distortion of density out of this plane. The asymmetry in the hydration of the ceramide amide group stems from the orientation of the amide relative to the bilayer, which is a result of the conformational constraint of having the tails directed towards the center of the bilayer.

Whilst the solution simulations provide important insight into the hydration of these lipids, ultimately the specific environment in which the lipid finds itself is likely to have an effect on the more subtle aspects of the hydration. The solution simulations provide a very good representation of the distance range at which the water molecules are likely to be located and the orientations at which they are likely to be found, but the more subtle aspects of the hydration such as the quantitative determination of the level of hydration and the exact location of the water in three-dimensional space is not so easy to capture. These more subtle aspects of hydration are likely to be highly dependent on the specific local environment and as such will vary between very similar systems. The incorporation of the lipid into the bilayer seems to be an important step, as the restricted conformations of the lipid molecules have a marked effect on hydration. The specific details of the local environment, such as changing the lipid composition of the bilayer or the inclusion of proteins, are likely to play a less significant role in determining the exact nature of the hydration pattern.

## ACKNOWLEDGMENTS

The authors thank the Engineering and Physical Sciences Research Council (Grant No. EP/J002615/1) for funding. Through our membership within the UK HPC Materials Chemistry Consortium, which is funded by the Office of Science and Technology through the EPSRC High End Computing Programme (Grant No. EP/L000202), the facilities of ARCHER, the UK National Supercomputing Service (<http://www.archer.ac.uk>), were used for the MD aspects of this work.

<sup>1</sup>S. J. Singer and G. L. Nicolson, "The fluid mosaic model of the structure of cell membranes," *Science* **175**, 720–731 (1972).

<sup>2</sup>G. van Meer, D. R. Voelker, and G. W. Feigenson, "Membrane lipids: Where they are and how they behave," *Nat. Rev. Mol. Cell Biol.* **9**, 112–124 (2008).

<sup>3</sup>G. S. Attard, R. H. Templer, W. S. Smith, A. N. Hunt, and S. Jackowski, "Modulation of CTP: Phosphocholine cytidyltransferase by membrane

curvature elastic stress," *Proc. Natl. Acad. Sci. U. S. A.* **97**, 9032–9036 (2000).

<sup>4</sup>P. L. Yeagle, "Lipid regulation of cell membrane structure and function," *FASEB J.* **3**, 1833–1842 (1989).

<sup>5</sup>Y. A. Hannun and L. M. Obeid, "Principles of bioactive lipid signalling: Lessons from sphingolipids," *Nat. Rev. Mol. Cell Biol.* **9**, 139–150 (2008).

<sup>6</sup>A. Zarbock, M. R. Distasi, E. Smith, J. M. Sanders, G. Kronke, B. L. Harry, S. von Vietinghoff, K. Buscher, J. L. Nadler, and K. Ley, "Improved survival and reduced vascular permeability by eliminating or blocking 12/15-lipoxygenase in mouse models of acute lung injury (ALI)," *J. Immunol.* **183**, 4715–4722 (2009).

<sup>7</sup>M. A. C. Bermingham, W. A. Boggust, and R. A. Q. O'Meara, "Lipids and phospholipids in blood coagulation," *Nature* **218**, 695–696 (1968).

<sup>8</sup>R. F. Zwaal, P. Comfurius, and E. M. Bevers, "Lipidprotein interactions in blood coagulation," *Biochim. Biophys. Acta* **1376**, 433–453 (1998).

<sup>9</sup>S. P. Srivastava, S. Shi, D. Koya, and K. Kanasaki, "Lipid mediators in diabetic nephropathy," *Fibrog. Tissue Repair* **7**, 12 (2014).

<sup>10</sup>J. Yang, H. Dong, and B. D. Hammock, "Profiling the regulatory lipids: Another systemic way to unveil the biological mystery," *Curr. Opin. Lipidol.* **22**, 197–203 (2011).

<sup>11</sup>J. Milhaud, "New insights into water-phospholipid model membrane interactions," *Biochim. Biophys. Acta* **1663**, 19–51 (2004).

<sup>12</sup>S. K. Balasubramanian, W. F. Wolters, and J. C. Bischof, "Membrane hydration correlates to cellular biophysics during freezing in mammalian cells," *Biochim. Biophys. Acta* **1788**, 945–953 (2009).

<sup>13</sup>P. Jurkiewicz, A. Olżyńska, M. Langner, and M. Hof, "Headgroup hydration and mobility of DOTAP/DOPC bilayers: A fluorescence solvent relaxation study," *Langmuir* **22**, 8741–8749 (2006).

<sup>14</sup>H.-C. Huang and T.-M. Chang, "Ceramide 1 and ceramide 3 act synergistically on skin hydration and the transepidermal water loss of sodium lauryl sulfate-irritated skin," *Int. J. Dermatol.* **47**, 812–819 (2008).

<sup>15</sup>K. S. Wu, W. W. van Osdol, and R. H. Dauskardt, "Mechanical properties of human stratum corneum: Effects of temperature, hydration, and chemical treatment," *Biomaterials* **27**, 785–795 (2006).

<sup>16</sup>A. Tfayli, D. Jamal, R. Vyumvuhore, M. Manfait, and A. Baillet-Luffroy, "Hydration effects on the barrier function of stratum corneum lipids: Raman analysis of ceramides 2, III and 5," *The Analyst* **138**, 6582–6588 (2013).

<sup>17</sup>E. Sparr, L. Hallin, N. Markova, and H. Wennerström, "Phospholipid-cholesterol bilayers under osmotic stress," *Biophys. J.* **83**, 2015–2025 (2002).

<sup>18</sup>K. J. Seu, L. R. Cambrea, R. M. Everly, and J. S. Hovis, "Influence of lipid chemistry on membrane fluidity: Tail and headgroup interactions," *Biophys. J.* **91**, 3727–3735 (2006).

<sup>19</sup>K. Gounaris, D. Mannock, A. Sen, A. Brain, W. Williams, and P. Quinn, "Polyunsaturated fatty acyl residues of galactolipids are involved in the control of bilayer/non-bilayer lipid transitions in higher plant chloroplasts," *Biochim. Biophys. Acta, Biomembr.* **732**, 229–242 (1983).

<sup>20</sup>J. Seelig, P. M. MacDonald, and P. G. Scherer, "Phospholipid head groups as sensors of electric charge in membranes," *Biochemistry* **26**, 7535–7541 (1987).

<sup>21</sup>Z. E. Hughes, A. E. Mark, and R. L. Mancera, "Molecular dynamics simulations of the interactions of DMSO with DPPC and DOPC phospholipid membranes," *J. Phys. Chem. B* **116**, 11911–11923 (2012).

<sup>22</sup>S. D. Campbell, K. J. Regina, and E. D. Kharasch, "Significance of lipid composition in a blood-brain barrier-mimetic PAMPA assay," *J. Biomol. Screening* **19**, 437–444 (2014).

<sup>23</sup>H. Takamura, H. Kasai, H. Arita, and M. Kito, "Phospholipid molecular species in human umbilical artery and vein endothelial cells," *J. Lipid Res.* **31**, 709–717 (1990).

<sup>24</sup>D. Hishikawa, T. Hashidate, T. Shimizu, and H. Shindou, "Diversity and function of membrane glycerophospholipids generated by the remodeling pathway in mammalian cells," *J. Lipid Res.* **55**, 799–807 (2014).

<sup>25</sup>S. Wartewig and R. H. H. Neubert, "Properties of ceramides and their impact on the stratum corneum structure: a review. Part 1. Ceramides," *Skin Pharmacol. Physiol.* **20**, 220–229 (2007).

<sup>26</sup>R. N. Kolesnick and S. Clegg, "1,2-Diacylglycerols, but not phorbol esters, activate a potential inhibitory pathway for protein kinase C in GH3 pituitary cells. Evidence for involvement of a sphingomyelinase," *J. Biol. Chem.* **263**, 6534–6537 (1988).

<sup>27</sup>F.-X. Contreras, G. Basañez, A. Alonso, A. Herrmann, and F. M. Goñi, "Asymmetric addition of ceramides but not dihydroceramides promotes transbilayer (flip-flop) lipid motion in membranes," *Biophys. J.* **88**, 348–359 (2005).



- <sup>28</sup>V. Filippov, M. A. Song, K. Zhang, H. V. Vinters, S. Tung, W. M. Kirsch, J. Yang, and P. J. Duerksen-Hughes, "Increased ceramide in brains with Alzheimer's and other neurodegenerative diseases," *J. Alzheimer's Dis.* **29**, 537–547 (2012).
- <sup>29</sup>M. Kosicek and S. Hecimovic, "Phospholipids and Alzheimer's disease: Alterations, mechanisms and potential biomarkers," *Int. J. Mol. Sci.* **14**, 1310–1322 (2013).
- <sup>30</sup>R. J. Gillams, J. V. Busto, S. Busch, F. M. Goñi, C. D. Lorenz, and S. E. McLain, "Solvation and hydration of the ceramide headgroup in a non-polar solution," *J. Phys. Chem. B* **119**, 128–139 (2015).
- <sup>31</sup>F. Foglia, M. J. Lawrence, C. D. Lorenz, and S. E. McLain, "On the hydration of the phosphocholine headgroup in aqueous solution," *J. Chem. Phys.* **133**, 145103 (2010).
- <sup>32</sup>A. P. Dabkowska, M. J. Lawrence, S. E. McLain, and C. D. Lorenz, "On the nature of hydrogen bonding between the phosphatidylcholine headgroup and water and dimethylsulfoxide," *Chem. Phys.* **410**, 31–36 (2013).
- <sup>33</sup>A. P. Dabkowska, L. E. Collins, D. J. Barlow, R. Barker, S. E. McLain, M. J. Lawrence, and C. D. Lorenz, "Modulation of dipalmitoylphosphatidylcholine monolayers by dimethyl sulfoxide," *Langmuir* **30**, 8803–8811 (2014).
- <sup>34</sup>S. Plimpton, "Fast parallel algorithms for short-range molecular dynamics," *J. Comput. Phys.* **117**, 1–19 (1995).
- <sup>35</sup>J. B. Klauda, R. M. Venable, J. A. Freites, J. W. O'Connor, D. J. Tobias, C. Mondragon-Ramirez, I. Vorobyov, A. D. MacKerell, and R. W. Pastor, "Update of the CHARMM all-atom additive force field for lipids: validation on six lipid types," *J. Phys. Chem. B* **114**, 7830–7843 (2010).
- <sup>36</sup>S. Guo, T. C. Moore, C. R. Iacovella, L. A. Strickland, and C. McCabe, "Simulation study of the structure and phase behavior of ceramide bilayers and the role of lipid headgroup chemistry," *J. Chem. Theory Comput.* **9**, 5116–5126 (2013).
- <sup>37</sup>W. L. Jorgensen, J. Chandrasekhar, J. D. Madura, R. W. Impey, and M. L. Klein, "Comparison of simple potential functions for simulating liquid water," *J. Chem. Phys.* **79**, 926–935 (1983).
- <sup>38</sup>W. I. Reiher, "Theoretical studies of hydrogen bonding," Ph.D. thesis, Harvard University (1985).
- <sup>39</sup>T. K. M. Nyholm, D. Lindroos, B. Westerlund, and J. P. Slotte, "Construction of a DOPC/PSM/cholesterol phase diagram based on the fluorescence properties of trans-parinaric acid," *Langmuir* **27**, 8339–8350 (2011).
- <sup>40</sup>J. B. Massey, "Interaction of ceramides with phosphatidylcholine, sphingomyelin and sphingomyelin/cholesterol bilayers," *Biochim. Biophys. Acta, Biomembr.* **1510**, 167–184 (2001).
- <sup>41</sup>Y.-W. Hsueh, R. Giles, N. Kitson, and J. Thewalt, "The effect of ceramide on phosphatidylcholine membranes: A deuterium NMR study," *Biophys. J.* **82**, 3089–3095 (2002).
- <sup>42</sup>J.-P. Ryckaert, G. Cicciotti, and H. J. Berendsen, "Numerical integration of the cartesian equations of motion of a system with constraints: Molecular dynamics of n-alkanes," *J. Comput. Phys.* **23**, 327–341 (1977).
- <sup>43</sup>R. W. Hockney and J. W. Eastwood, *Computer Simulation Using Particles* (Taylor and Francis Group, New York, 1988), p. 540.
- <sup>44</sup>L. C. Pardo, "ANGULA," <https://gcm.upc.edu/en/members/luis-carlos/angula/ANGULA>, last accessed 15 December 2015.
- <sup>45</sup>M. Rovira-Esteva, N. A. Murugan, L. C. Pardo, S. Busch, J. L. Tamarit, G. J. Cuello, and F. J. Bermejo, "Differences in first neighbor orientation behind the anomalies in the low and high density trans-1,2-dichloroethene liquid," *J. Chem. Phys.* **136**, 124514 (2012).
- <sup>46</sup>F. Perez and B. E. Granger, "IPython: A system for interactive scientific computing," *Comput. Sci. Eng.* **9**, 21–29 (2007).
- <sup>47</sup>P. Ramachandran and G. Varoquaux, "Mayavi: 3D visualization of scientific data," *Comput. Sci. Eng.* **13**, 40–51 (2011).
- <sup>48</sup>S. Busch, C. D. Lorenz, J. Taylor, L. C. Pardo, and S. E. McLain, "Short-range interactions of concentrated proline in aqueous solution," *J. Phys. Chem. B* **118**, 14267–14277 (2014).
- <sup>49</sup>A. J. Johnston, Y. R. Zhang, S. Busch, L. C. Pardo, S. Imberti, and S. E. McLain, "Amphipathic solvation of indole: Implications for the role of tryptophan in membrane proteins," *J. Phys. Chem. B* **119**, 5979–5987 (2015).
- <sup>50</sup>V. Gapsys, B. L. de Groot, and R. Briones, "Computational analysis of local membrane properties," *J. Comput.-Aided Mol. Des.* **27**, 845–848 (2013).
- <sup>51</sup>E. Falck, M. Patra, M. Karttunen, M. T. Hyvönen, and I. Vattulainen, "Lessons of slicing membranes: Interplay of packing, free area, and lateral diffusion in phospholipid/cholesterol bilayers," *Biophys. J.* **87**, 1076–1091 (2004).
- <sup>52</sup>O. Edholm and J. F. Nagle, "Areas of molecules in membranes consisting of mixtures," *Biophys. J.* **89**, 1827–1832 (2005).
- <sup>53</sup>R. Guixà-González, I. Rodríguez-Espigares, J. M. Ramírez-Anguaita, P. Carrió-Gaspar, H. Martínez-Seara, T. Giorgino, and J. Selent, "MEMB-PLUGIN: Studying membrane complexity in VMD," *Bioinformatics* **30**, 1478–1480 (2014).
- <sup>54</sup>F. M. Goñi and A. Alonso, "Biophysics of sphingolipids I. Membrane properties of sphingosine, ceramides and other simple sphingolipids," *Biochim. Biophys. Acta* **1758**, 1902–1921 (2006).
- <sup>55</sup>A. K. Soper, "The excluded volume effect in confined fluids and liquid mixtures," *J. Phys.: Condens. Matter* **9**, 2399–2410 (1997).
- <sup>56</sup>E. C. Hulme, A. K. Soper, S. E. McLain, and J. L. Finney, "The hydration of the neurotransmitter acetylcholine in aqueous solution," *Biophys. J.* **91**, 2371–2380 (2006).
- <sup>57</sup>N. H. Rhys, A. K. Soper, and L. Dougan, "Hydrophilic association in a dilute glutamine solution persists independent of increasing temperature," *J. Phys. Chem. B* **119**, 15644–15651 (2015).
- <sup>58</sup>J. F. Nagle and S. Tristram-Nagle, "Lipid bilayer structure," *Curr. Opin. Struct. Biol.* **10**, 474–480 (2000).
- <sup>59</sup>E. A. Disalvo, F. Lairion, F. Martini, E. Tymczyszyn, M. Frías, H. Almaleck, and G. J. Gordillo, "Structural and functional properties of hydration and confined water in membrane interfaces," *Biochim. Biophys. Acta* **1778**, 2655–2670 (2008).
- <sup>60</sup>See supplementary material at <http://dx.doi.org/10.1063/1.4952444> for more detailed analysis and further information on analysis methods.